Localization of auroral Langmuir turbulence in thin layers

H. Akbari,[1] J. L. Semeter,[1] M. J. Nicolls,[2] M. Broughton,[3] and J. W. LaBelle[3]

Received 3 January 2013; revised 30 April 2013; accepted 2 May 2013; published 6 June 2013.

[1] The recently discovered coherent echoes in the Poker Flat Incoherent Scatter Radar data with flat ion-line spectrum and simultaneous double-peaked plasma-line spectrum in the lower ionospheric *F* region are investigated in greater detail. High-range resolution measurements reveal that the turbulence is sometimes manifested as two concurrent layers separated by about 50 km. The turbulence layers appear at regions of zero electron density gradient, supporting the interpretation that propagation effects play an important role in limiting the waves' amplitude. Although Langmuir intensity is limited by propagation effects outside of the layers, it reaches to nonlinear regime inside the layers, giving rise to the observed range and spectral morphologies. Furthermore, the radar measurements of the electrostatic waves appear to be correlated in space and time with natural auroral electromagnetic emissions, supporting the previous theory that "MF-bursts" are produced by linear conversion of Langmuir waves produced by soft electron precipitation (~few hundred electronvolts) on the topside *F* region. The results presented in this report suggest that the observed Langmuir turbulence and MF-burst are both manifestations of the same process.

Citation: Akbari, H., J. L. Semeter, M. J. Nicolls, M. Broughton, and J. W. LaBelle (2013), Localization of auroral Langmuir turbulence in thin layers, *J. Geophys. Res. Space Physics*, *118*, 3576–3583, doi:10.1002/jgra.50314.

1. Introduction

[2] Incoherent scatter radars (ISRs) are designed to sense the weak thermal fluctuations in the ionospheric plasma, and as such are highly sensitive to plasma instabilities and the coherent structures they produce. At high latitudes, magnetic field-aligned electron beams commonly drive the ionosphere out of stability, creating different signatures in the radar data. One example is the well-known naturally enhanced ion acoustic lines, in which one or sometimes both shoulders of the ion-line spectrum are enhanced above the thermal level [*Sedgemore-Schulthess and St. Maurice*, 2001; *Michell and Samara*, 2010]. Recently, a new type of signature has been observed with the Poker Flat Incoherent Scatter Radar (PFISR) [*Akbari et al*., 2012]. These signatures are characterized by a simultaneous enhancement of the ion-line and the plasma-line spectra in which the ion-line spectrum is flat and the plasma-line spectrum sometimes contains two peaks in both the up- and down-shifted channels (see Figure 1). *Akbari et al*. [2012] and *Isham et al*. [2012] have argued that such signatures are manifestations of naturally occurring cavitating Langmuir turbulence produced by auroral processes in the *F* region ionosphere.

[3] Whether the observed Langmuir turbulence (LT) is in cascading or cavitating regime is not the focus of this paper. This report seeks to clarify the role of an important factor—the background density gradient—in the development of the natural LT using examples recorded by the 450 MHz PFISR facility. Of particular interest are alternating code (AC) measurements of enhanced ion-line spectra at 4.5 km range resolution. Alternating codes [*Lehtinen*, 1986] are sets of phase-coded pulses that permit spectral measurements with high range resolution at the expense of lower SNR. The AC measurements reveal that the natural turbulence is sometimes manifested as two concurrent layers. Interestingly, the turbulence layers are located in regions with zero vertical density gradients. These events appear in conjunction with natural electromagnetic emissions known as "MF-bursts", also thought to be caused by mode conversion of unstable Langmuir waves.

2. Observations

[4] Figure 1, from *Akbari et al*. [2012], shows plasma-line and ion-line spectra observed with the PFISR on 23 March 2007. The observed features were confined to a thin layer (~10 km) centered at ~230 km altitude and occurred on the edge of the auroral activity during the expansion phase of a substorm. The double-peaked plasma line (Figure 1a) can be explained by the cavitating LT theory where the lower frequency peak, at the plasma frequency, is due to scattering of the radar wave by Langmuir waves trapped in density wells (cavitons), and the higher frequency peak at the Langmuir frequency, is due to scattering of the radar wave by the "free modes", i.e., Langmuir waves present in the background plasma. This interpretation is supported by our calculations of plasma frequency and Langmuir frequency.

[1]Department of Electrical and Computer Engineering and Center for Space Physics, Boston University, Boston, Massachusetts, USA.
[2]SRI International, Menlo Park, California, USA.
[3]Department of Physics and Astronomy, Dartmouth College, Hanover, New Hampshire, USA.

Corresponding author: H. Akbari, Department of Electrical and Computer Engineering and Center for Space Physics, Boston University, 8 Saint Mary's St., Boston, MA 02215, USA. (hakbari@bu.edu)

2169-9380/13/10.1002/jgra.50314

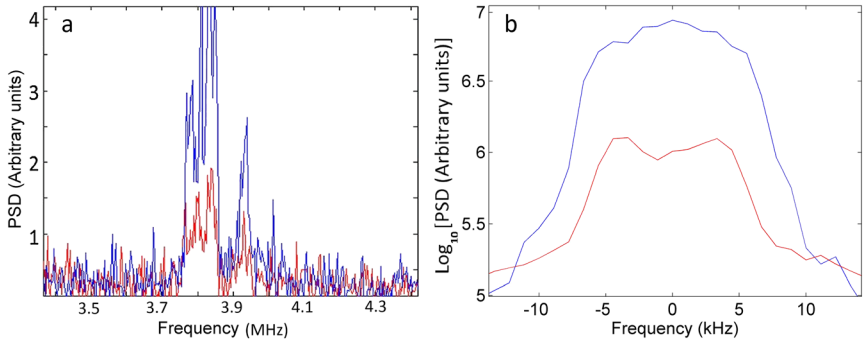

Figure 1. (a) Double-peaked plasma line in down-shifted (blue) and up-shifted channel (red) observed on 23 March 2007; manifested as the naturally occurring cavitating Langmuir turbulence (negative frequencies are folded on top of the positive frequencies). (b) Blue: ion-line spectrum corresponding to the plasma line on the left panel and red: typical thermal double-humped ion-line spectrum.

By performing the standard ISR fitting procedure, we derive the background electron density of $n_e = 1.82 \times 10^{11}$ [m^{-3}] and the plasma frequency of $f_p = 3.83$ MHz, which agrees with the position of the first peak in our plasma line measurement. The background electron temperature is calculated to be 1925K, and the angle between the radar beam and the magnetic field lines at 230 km is about 1.148°. Substituting these into the linear Langmuir dispersion relation gives the Langmuir frequency of 3.93 MHz, which is close to the position of the second peak in our experiment (3.939 MHz). In the ion line (Figure 1b), the observed flat spectrum can be explained by the existence of an additional peak at zero Doppler and its superposition with the thermal double-humped spectrum. The central peak is interpreted as Bragg scatter of the radar wave from the nonpropagating density wells (cavities) [*DuBois et al.*, 1990]. Similar signatures are commonly observed during ionospheric heating experiments, where a heater wave provides the energy for the Langmuir turbulence [*Stubbe et al.*, 1992; *Isham et al.*, 1999; *Cheung et al.*, 1989; *Birkmayer et al.*, 1986]. It is important to note that here the argument for the cavitating nature of the turbulence is the observation of the double-peaked plasma-line spectra and the ion-line morphologies together and not the ion-line morphology solely.

[5] Figure 2 compares representative ion-line power spectra associated with natural turbulence (Figure 2a) and heater-induced turbulence (Figure 2b), both observed with PFISR. The heater-induced turbulence was generated by the High Power Auroral Stimulation heater, which was located ~35 km from PFISR [*Kosch et al.*, 2009]. In each case, the spectra were calculated using a 72 km long pulse. Thus, even though the turbulence is confined to thin layers, the backscattered power is seen over an extended altitude range. The two panels are different in that in the heater-produced turbulence, unlike the naturally produced case, the central peak is distinguishable from the ion acoustic peaks. The origin of the difference is not clear at this point but it might be due to the different nature of the source in the two cases. Another difference is the stronger incoherent scattering from the *E* region (100–150 km) in the case of the natural turbulence due to density enhancement produced by electron precipitation.

[6] In an attempt to collect more information about the underlying processes responsible for these signatures, we have studied 3 months of the PFISR data, from January 2012 to April 2012. The data include ion- and plasma-line measurements from a 480 μs long pulse, and ion-line measurements from a 16 baud AC. Although different radar beam patterns were used in the various experiments, we focus only on observations

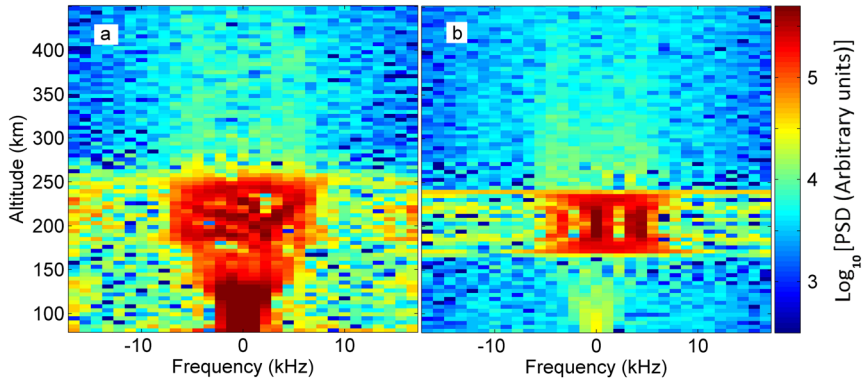

Figure 2. PFISR observations of anomalous ion-line spectra from (a) naturally and (b) heater wave produced Langmuir turbulence. Figure 2a corresponds to the data shown in Figure 1. Figure 2b was recorded during an active ionospheric modification experiment using the High Power Auroral Stimulation facility 17 March 2007.

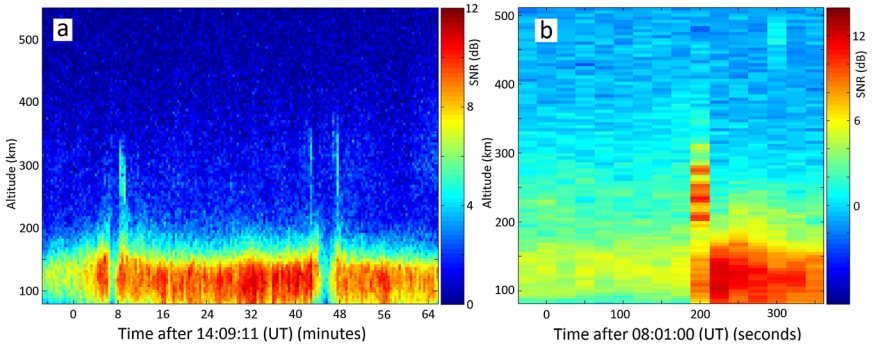

Figure 3. Received radar power in the ion-line channel as a function of altitude and time, showing occurrences of coherent scatter just outside of periods of *E* region ionization enhancement due to electron precipitation (left, 20 February 2012; right, 27 January 2012).

from the magnetic zenith beam (154.3° azimuth, 77.5° elevation), where the largest coherent echoes were observed.

[7] Our search through the PFISR database resulted in identifying 35 instances of coherent scatter exhibiting flat ion-line spectra similar to Figure 2a. The enhanced scatter usually appeared in thin layers (<10 km) at or close to the *F* region peak, and occurred just before the *E* region ionization maximized due to the electron precipitation. Figure 3 shows two example range-time-intensity plots illustrating the temporal relationship between enhanced ion line power (echoes above 200 km) and *E* region ionization associated with the visible aurora (echoes below 150 km). Correlating these data with optical data confirms that the sudden drops in the *E* region signal strength correspond to sudden drops in intensity of aurora luminosity within the radar beam field of view. This does not necessarily imply that the electron precipitation has stopped in this period; however, this suggests a change in the energy of the precipitating electrons. This observation together with occurrence of the radar echoes on the edge of the aurora suggest soft electron precipitations as the source of the echoes, because the vicinity of an auroral arc is an ideal place for such electrons [*Mishin and Banaszkiewicz*, 1998; *Arnoldy et al*., 1999]. The duration of the enhanced scatter is typically only a few seconds in the radar frame of reference. One fortuitous event, highlighted below, endured in the radar beam for over 5 min.

[8] In only 11 of our 35 cases were ion-line enhancements accompanied by plasma-line enhancements in either or both the up- and down-shifted channels, and in only three cases were double-peaked plasma lines observed. According to Bragg scattering principle a radar only observes a single spatial frequency component *k*, and so simultaneous observation of Langmuir turbulence in the plasma line and the ion line is only possible if some conditions on intensity and bandwidth of the source are met [*Diaz et al*., 2010]. However, in cavitating LT, regardless of the spread in the beam velocity, collapse and dissipation lead to Langmuir wave enhancement over a broad *k*-space [*Guio and Forme*, 2006; *Goldman*, 1984; *Robinson*, 1997] and thus one would expect to observe the plasma-line enhancement in more than 11 examples. Although Langmuir turbulence is only one of the processes capable of producing ion acoustic wave enhancement, based on the similar characteristics of the echoes with double-peaked plasma-line spectra and those not accompanied by plasma-line enhancements, i.e., (1) occurrence of the echoes in thin layers close to the *F* region peak and (2) flat or filled-in ion-line spectra, we reasonably conclude that all the observed echoes are manifestation of Langmuir turbulence. Here we focus our presentation on the morphology of the ion lines, which are a more sensitive and ubiquitous indicator of the presence of turbulence.

[9] Figure 4a plots ion-line power from AC measurements on 5 April 2012 at around 7:00 UT. The turbulence is manifested as thin layers of coherent scatter at 260 and 210 km. The upper layer persisted in the radar beam for over 5 min, and the lower layer for almost 1 min. This provided

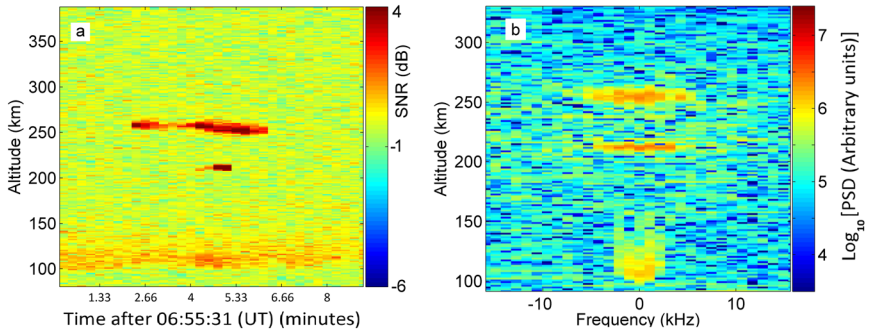

Figure 4. (a) Ion-line power profile from alternating codes, showing localization of the turbulence in two thin layers. (b) Ion-line power spectrum corresponding to Figure 4a, integrated between 4.5 and 5.33 min (data from 5 April 2012).

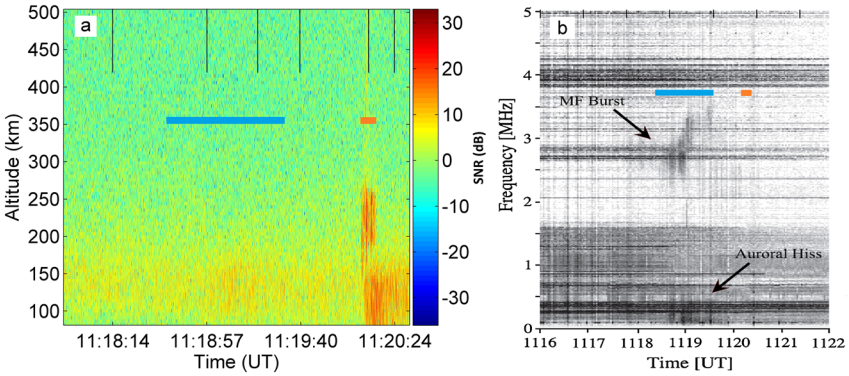

Figure 5. (a) Ion-line power profile: occurrence of the coherent scatter at 11:20:08 UT, 23 March 2007. (b) Spectrogram of natural electromagnetic emissions accompanying the auroral activity, recorded with the base antenna at Toolik Lake (plot taken from *Bunch et al*. [2008]). The blue and the orange bars specify the time of the features in each panel.

sufficient statistics to compute ion line spectra within the turbulence layers at 4.5 km range resolution. Figure 4b shows the ion-line power spectrum integrated between 4.5 and 5.33 min. The spectra in both layers are similar to Figure 2a, but with the altitude smearing removed. Only the upper layer is accompanied by plasma line enhancement. Such double-layer profile was observed in 6 cases out of 35.

[10] Figure 5a shows the ion-line power profile for the LT event reported by *Akbari et al*. [2012]. Figure 5b, from *Bunch et al*. [2008], shows a 0–5 MHz spectrogram of electromagnetic emissions accompanying the auroral activity, recorded with the base antenna at Toolik Lake (about 400 km to the north of PFISR). The horizontal lines are man-made interference signals. The emission labeled "MF-burst" is one type of auroral electromagnetic (EM) emissions detectable at ground [*Weatherwax et al*., 1994; *Kellogg and Monson*, 1979, 1984; *Bale*, 1999]. Coincident with the MF-burst, the Toolik receiver also records auroral hiss, a broadband impulsive emission at frequencies below 500 kHz [for a review on auroral EM emissions look at *LaBelle and Treumann*, 2002]. Using a ray tracing technique, *Bunch et al*. [2008] showed that the MF-burst originates about 400 km south of the receiver at Toolik Lake, at the approximate location of the PFISR. The orange and the blue bars on Figures 5a and 5b show the time periods when the electrostatic turbulence and the MF-burst, respectively, happen.

[11] For context, Figure 6 shows a sequence of all-sky camera images recorded from Fort Yukon, AK, during this interval. The observations occurred during a substorm expansion phase, with onset point a few hundred kilometers to the west of PFISR at ~11:18 UT [*Angelopoulos et al*., 2008]. The image sample times are indicated by vertical black lines in Figure 5a, and the PFISR location is indicated by a red circle in Figure 6. The onset of LT corresponded with an auroral brightening and subsequent breakup at ~11:20UT (Figures 6d–6f). Analysis of high-speed imagery from Poker Flat at this time suggests the presence of dispersive-scale Alfvén waves within the PFISR beam [*Semeter and Blixt*, 2006; *Semeter et al*., 2008]. Nonlinear evolution of inertial Alfvén waves provides one mechanism for producing the high-density, low-energy electron beams required for inducing cavitating Langmuir turbulence [*Mishin and Banaszkiewicz*, 1998; *Mishin and Förster*, 1995].

[12] Figure 7, in the same format as Figure 5, shows another example of simultaneous measurements of PFISR echoes and natural EM emissions recorded at Toolik Lake. Four types of EM emissions occur sporadically during the approximately 1 h interval shown in Figure 7b: $2f_{ce}$ and $3f_{ce}$ auroral roars, which are narrowband emissions near 2.9 and 4.0 MHz presumed to result from upper hybrid waves; auroral hiss at frequencies below 1 MHz; and auroral MF-burst, including four bursts exceeding 2 min duration and spanning approximately 2.9–3.3 MHz. Two of the three radar echoes detected with the PFISR, centered approximately at 8:49 and 9:03 UT, coincide with two of the four MF-bursts. In the latter case, auroral hiss occurs at the same time as well. The probability of these coincidences happening by chance is about 5%; this level of coincidence is all the more surprising considering that Toolik Lake is located more than 400 km from the PFISR, and MF-burst occurrence at ground level is severely affected by propagation effects in the disturbed auroral ionosphere.

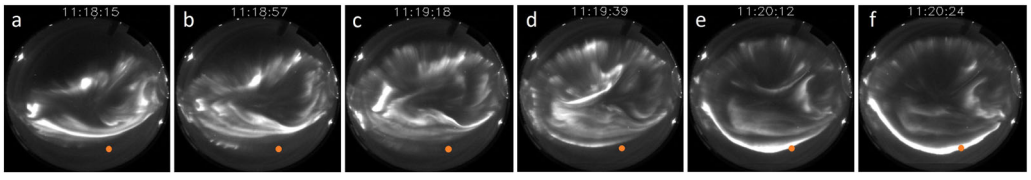

Figure 6. A sequence of all-sky camera images recorded from Fort Yukon, AK. The image sample times are indicated by vertical black lines in Figure 5a, and the PFISR location is indicated by a red circle in Figure 6.

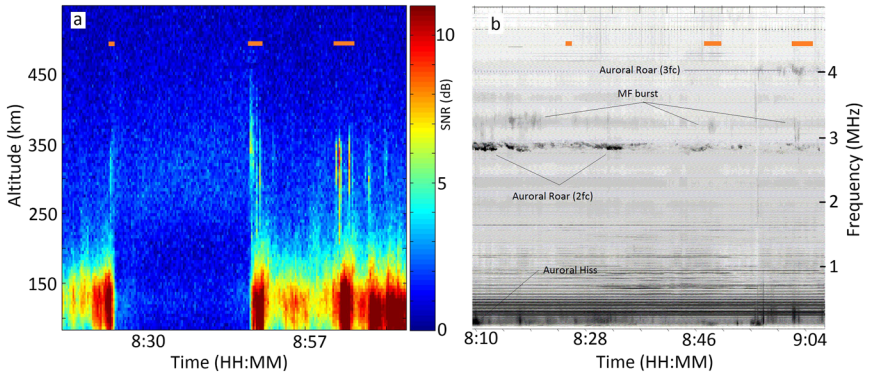

Figure 7. Similar to Figure 5: (a) ion-line power profile and (b) spectrogram of natural electromagnetic emissions. For convenience the time interval of three coherent scatters are marked by orange bars in both panels. (Data from 5 April 2012).

3. Discussion

[13] Typically, magnetospheric electron beams are assumed to be directly responsible for the ionospheric turbulences and their signatures in radar data. Electron beams are expected to interact with the ionosphere in an extended altitude range and thus are not consistent with the localization of the radar echoes in thin layers. A careful examination of the PFISR data reveals that this localization cannot be explained as an ISR wave number matching effect. Enhancement of both up- and down-shifted plasma lines at wave number $k = 20$ (the spatial frequency component observable by the PFISR) requires parametric decay of either up- or down-going Langmuir waves at wave number $k \approx 20$. On the other hand, enhancement of ion acoustic lines at wave number $k = 20$ requires parametric decay of Langmuir waves with wave number $k \approx 10$. This broad enhancement in k-space, at a single altitude, implies a large velocity spread and/or a large intensity of the electron beam which, in turn, guarantees that the PFISR wave number matching conditions are met over an altitude range that far exceeds the width of the observed turbulence layer. In an extreme case, it is possible that the highest wave number of the enhanced Langmuir waves in the top layer is $k = 20$; as the beam propagates downward to a region of lower plasma density, it amplifies Langmuir waves at lower wave numbers ($k < 20$). Such waves are invisible to the radar and consequently the radar only sees a localized plasma-line enhancement. However, given the large velocity spread of the beam, ion acoustic waves produced by parametric decay of such invisible Langmuir waves should be visible to the radar. Therefore, we conclude that the observed localization of the ion-line enhancement in thin layers implies localization of the turbulence.

[14] Several mechanisms have been proposed that can lead to localization of turbulence in thin layers. *Mishin and Schlegel* [1994] used the theory of plasma turbulence layer to explain, ISR observations of intense Langmuir wave enhancements within layers with altitude extent less than the ionospheric scale heights in auroral E region. This mechanism requires relatively sharp variation of collision frequency with altitude and thus is not applicable to our F region observations. Plasma waves being trapped in small-scale (order km) density cavities or enhancements are also proposed to explain some rocket observations of intense localized wave enhancements [*McAdams et al.*, 2000; C. W. Carlson et al., Observations of intense electron Bernstein wave emissions in an auroral plasma, unpublished manuscript, 1987]. Amplification of plasma waves not only depends on the growth rate, which is mainly determined by the source characteristics, i.e., auroral electron distribution function, but also

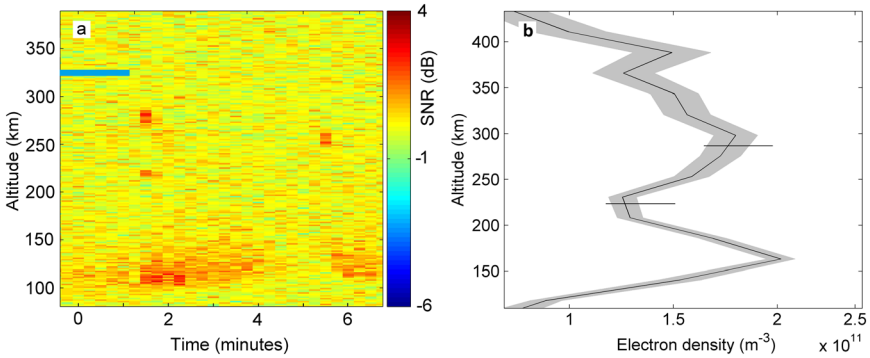

Figure 8. (a) Ion line power profile from the alternating codes, showing the localization of turbulence in two thin layers. (b) Background electron density profile averaged over the incoherent scatter measurement period marked by the blue bar in the left panel. Shaded area represents the statistical accuracy of the measurements (one standard deviation). The two horizontal bars show the location of the two layers with respect to the background density. (Data from 17 March 2012).

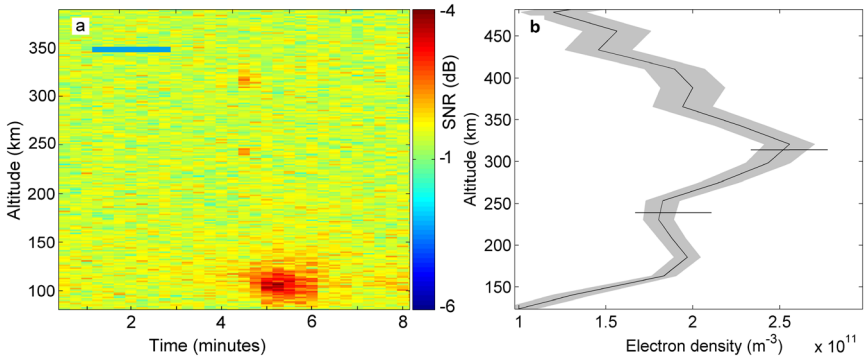

Figure 9. Similar to Figure 8, (a) another example of double-layer profile observed in the ion line channel and (b) locations of the layers with respect to the background electron density. (Data from 5 April 2012).

depends on growth time—i.e., the time period in which the wave stays resonant with the source, which is typically determined by the ambient plasma and the wave's dispersion relation. In the auroral ionosphere, often latter is the critical factor that limits the wave amplification [*Maggs*, 1978; C. W. Carlson et al., unpublished manuscript, 1987]. In such situations, wave trapping in density enhancements or cavities provides further amplification by allowing the wave to stay resonant for a longer period. Short-scale density cavities capable of trapping the Langmuir waves cannot be resolved with our long range-resolution ISR data and therefore their possible roles in the localization of the turbulence in thin layers cannot be investigated.

[15] Similar to Figure 4a, Figures 8a and 9a present other examples of AC measurement of two turbulence layers. Also shown in each figure is the background electron density profile. The incoherent scatter measurement period that is used to calculate the density profiles are marked by the color bars in the left panels and the location of the turbulence layers with respect to the electron density profiles are specified by the horizontal bars on the right panels. The shaded area around the density profiles represents error bars and statistical accuracy of the calculations. Interestingly, the turbulence layers are located at regions of minimal density gradient, where the effect of propagation in limiting the Langmuir energy is minimum.

[16] In the presence of density gradient, propagation of Langmuir waves leads to change in the phase velocity and consequently detuning the waves from the electron beam and limiting the amplitude of the waves. Our calculations for altitudes between the two turbulence layers in Figure 8a, where the density gradient is highest with linear-scale height of ~200 km, shows that the Langmuir waves amplified by a down-going electron beam with energy of 100 eV and beam velocity spread of $\Delta v = 0.3v$, only propagate 500 m until they become off-resonant with the beam. Given the calculated 22.5 km/s group velocity of such waves, the total resonant time is about 22 ms. In fact the exact resonant time is even less. As the wave propagates down the density gradient its phase velocity decreases and the group velocity increases according to $v_g = 3KT_e/m_e v_\varphi$, decreasing the total resonant time. Here v_φ, m_e, K, and T_e are the wave's phase velocity, electron mass, Boltzmann constant, and electron temperature, respectively. Furthermore, during this time the wave is not being amplified by the highest possible growth rate. On the other hand, propagation of the Langmuir waves with constant group velocity of 22.5 km/s in a 5 km long region of zero density gradient, at the location of the turbulence layers, ensures that the waves remain resonant with the beam, with the highest possible growth rate, for at least 220 ms. The required resonant time for the Langmuir waves to reach the nonlinear regime depends on the growth rate and the beam parameters, however, for reasonable auroral electron beams and neglecting the propagation effects this time is in the order of tens of milliseconds [*Guio and Forme*, 2006]. Therefore, with such electron beams, propagation effects may be able to limit the Langmuir waves' amplitude in the regions between the two turbulence layers, preventing them from reaching the nonlinear regime. However, in the region of zero density gradient the Langmuir waves can reach to high intensities and develop the turbulence layers.

[17] In comparison with the 100 eV beam, Langmuir waves resonant with a lower energy beam need to propagate longer distances, in the same density gradient, to become off-resonant. For instance, for beams with mean energy of 20 and 4.6 eV and velocity spread of $\Delta v = 0.3v$ the resonant distances and times are, 3 and 12 km and 57 and 112 ms, respectively (calculated for linear-scale height of ~200 km). Therefore, for higher energy beams one would expect to observe enhancements more localized in altitude in ISR data. Note that in the case of higher energy beams (>20 eV) the mother Langmuir wave and Langmuir and ion acoustic waves produced by cascading Langmuir turbulence are all invisible to the radar, and observation of the turbulence with the radar requires a mechanism capable of transferring energy to higher wave numbers, i.e., cavitating Langmuir turbulence.

[18] MF-burst, an impulsive broadband emission at 1.3–4.5 MHz associated with the onset of auroral substorms, is one type of auroral EM emissions detectable at ground [*Weatherwax et al.*, 1994]. The generation mechanism of MF-bursts remains unclear, but the prevailing theory involves linear mode conversion of Langmuir or upper-hybrid waves driven by auroral electron beams or loss cone features over an extended altitude range on the bottom-side *F* region [*LaBelle et al.*, 1997, 2005]. Other theories involve nonlinear conversion of electron acoustic or electron cyclotron sound waves into broadband electromagnetic emissions [*Sotnikov et al.*, 1996; *Bunch et al.*, 2011]. *Bunch et al.* [2011] found all the mechanisms mentioned above to be viable based on consideration of conditions for resonance between auroral electrons and either wave mode.

[19] *LaBelle* [2011] considered another possibility, that MF-burst is produced by linear mode conversion of Langmuir waves, driven by low-energy beams (~few hundred eV) on the topside *F* region, to LO-mode. In this model, Langmuir waves propagate downward to regions of higher plasma density implying that their wave number decreases. After a short distance, Langmuir waves propagating parallel to magnetic field lines and linearly convert to downward propagating *L*-mode waves. Below the *F* region peak, the *L*-mode waves encounter decreasing plasma density as they propagate and their wave number increases. Upon reaching the conversion point some portion of the waves that propagate parallel to the magnetic field lines converts back to Langmuir waves and the rest freely propagate to the ground as MF-burst. In this model low-energy (< keV) electron beams are assumed as the energy source because they fit more properly with the shape of the fine structures present in MF-burst [*LaBelle*, 2011].

[20] In our data, simultaneous measurement of Langmuir turbulence and MF-burst, together with observation of the radar echoes on the edge of the auroral precipitations and just before onset of *E* region ionization enhancement, which are indications of the presence of low-energy beams (< 1 keV), provide evidence in support of the mechanism proposed by *LaBelle* [2011]. The offset in timing between the MF-burst and the UHF turbulence is not surprising given the dynamic nature of the event and the differences in fields-of-view and observing geometry for the two instruments.

4. Summary

[21] We argue that, for energy sources only marginally above the nonlinear regime threshold, propagation effects might play an important role in limiting the wave amplitude and development of turbulence. Localization of the radar echoes in thin layers at regions of zero background electron density gradient is strong evidence in support of our argument. Although effectiveness of propagation effects is more expected for higher energy beams, no definite conclusion about the beam parameters can be reached due to many degrees of freedom in the electron beam. Furthermore, simultaneous observation of Langmuir turbulence in the PFISR data and MF-burst supports the previous theory that MF-burst is produced by linear mode conversion of Langmuir waves enhanced by soft electron precipitations over extended altitude range on top-side *F* region.

[22] **Acknowledgments.** This work was supported by the National Science Foundation under grants 0852850 and 0608577. The Toolik Lake observations were supported by the National Science Foundation under grant AGS-1147699 to Dartmouth College.

References

Akbari, H., J. L. Semeter, H. Dahlgren, M. Diaz, M. Zettergren, A. Strømme, M. J. Nicolls, and C. Heinselman (2012), Anomalous ISR echoes preceding auroral breakup: Evidence for strong Langmuir turbulence, *Geophys. Res. Lett.*, *39*, L03102, doi:10.1029/2011GL050288.

Angelopoulos, V., et al. (2008), First Results from the THEMIS Mission, *Space Sci. Rev.*, *141*, 453–476.

Arnoldy, R. L., K. A. Lynch, J. B. Austin, and P. M. Kintner (1999), Energy and pitch angle-dispersed auroral electrons suggesting a time-variable, inverted-V potential structure, *J. Geophys. Res.*, *104*(A10), 22,613–22,621, doi:10.1029/1999JA900219.

Bale, S. D. (1999), Observation of topside ionospheric MF/HF radio emission from space, *Geophys. Res. Lett.*, *26*(6), 667–670.

Birkmayer, W., T. Hagfors, and W. Kofman (1986), Small-scale plasma-density depletions in Arecibo high-frequency modification experiments, *Phys. Rev. Lett.*, *57*, 1008–1011.

Bunch, N. L., J. LaBelle, A. T. Weatherwax, and J. M. Hughes (2008), Auroral medium frequency burst radio emission associated with the 23 March 2007 THEMIS study substorm, *J. Geophys. Res.*, *113*, A00C08, doi:10.1029/2008JA013503, [printed 115(A1), 2010].

Bunch, N. L., J. LaBelle, P. Yoon, and A. T. Weatherwax (2011), Theoretical constraints on the generation mechanism of auroral medium frequency burst radio emissions, *J. Geophys. Res.*, *116*, A01315, doi:10.1029/2010JA015951.

Cheung, P. Y., A. Y. Wong, T. Tanikawa, J. Santoru, D. F. DuBois, H. A. Rose, and D. Russell (1989), Short–time-scale evidence for strong Langmuir turbulence during hf heating of the ionosphere, *Phys. Rev. Lett.*, *62*, 2676.

Diaz, M. A., J. L. Semeter, M. Oppenheim, and M. Zettergren (2010), Analysis of beam plasma instability effects on incoherent scatter spectra, *Ann. Geophys.*, *28*, 2169–2175, doi:10.5194/angeo-28-2169-2010.

DuBois, D., H. Rose, and D. Russell (1990), Excitation of strong Langmuir turbulence in plasmas near critical density: Application to HF heating of the ionosphere, *J. Geophys. Res.*, *95*(A12), 21,221–21,272, doi:10.1029/JA095iA12p21221.

Goldman, M. V. (1984), Strong turbulence of plasma waves, *Rev. Mod. Phys.*, *56*, 709–735.

Guio, P., and F. Forme (2006), Zakharov simulations of Langmuir turbulence: Effects on the ion-acoustic waves in incoherent scattering, *Phys. Plasmas*, *13*, 122902, doi:10.1063/1.2402145.

Isham, B., C. La Hoz, M. T. Rietveld, T. Hagfors, and T. B. Leyser (1999), Cavitating Langmuir turbulence observed during high-latitude ionospheric wave interaction experiments, *Phys. Rev. Lett.*, *83*, 2576–2579, doi:10.1103/PhysRevLett.83.2576.

Isham, B., M. T. Rietveld, P. Guio, F. R. E. Forme, T. Grydeland, and E. Mjolhus (2012), Cavitating Langmuir Turbulence in the Terrestrial Aurora, *Phys. Rev. Lett.*, *108*, 105003, doi:10.1103/PhysRevLett.108.105003.

Kellogg, P. J., and S. J. Monson (1979), Radio emissions from the aurora, *Geophys. Res. Lett.*, *6*(4), 297–300, doi:10.1029/GL006i004p00297.

Kellogg, P. J., and S. J. Monson (1984), Further studies of auroral roar, *Radio Sci.*, *19*(2), 551–555, doi:10.1029/RS019i002p00551.

Kosch, M. J., et al. (2009), First incoherent scatter radar observations of ionospheric heating on the second electron gyro-harmonic, *J. Atmos. Solar-Terr. Phys.*, *71*, 1959–1966, doi:10.1016/j.jastp.2009.08.007.

LaBelle, J. (2011), An explanation for the fine structure of MF burst emissions, *Geophys. Res. Lett.*, *38*, L03105, doi:10.1029/2010GL046218.

LaBelle, J., and R. A. Treumann (2002), Auroral radio emissions. 1. Hisses, roars, and bursts, *Space Sci. Rev.*, *101*, 295–440, doi:10.1023/A:1020850022070.

LaBelle, J., S. G. Shepherd, and M. L. Trimpi (1997), Observations of auroral medium frequency bursts, *J. Geophys. Res.*, *102*(A10), 22,221–22,231, doi:10.1029/97JA01905.

LaBelle, J., A. T. Weatherwax, M. Tantiwiwat, E. Jackson, and J. Linder (2005), Statistical studies of auroral MF burst emissions observed at South Pole Station and at multiple sites in northern Canada, *J. Geophys. Res.*, *110*, A02305, doi:10.1029/2004JA010608.

Lehtinen, M. S. (1986), *Statistical theory of incoherent scatter radar measurements*, Tech. Rep. 86/45Eur. Incoherent Scatter Sci. Assoc., Kiruna, Sweden.

Maggs, J. E. (1978), Electrostatic noise generated by the auroral electron beam, *J. Geophys. Res.*, *83*(A7), 3173–3188, doi:10.1029/JA083iA07p03173.

McAdams, K. L., R. E. Ergun, and J. LaBelle (2000), Hf chirps: Eigenmode trapping in density depletions, *Geophys. Res. Lett.*, *27*(3), 321.

Michell, R. G., and M. Samara (2010), High-resolution observations of naturally enhanced ion acoustic lines and accompanying auroral fine structures, *J. Geophys. Res.*, *115*, A03310, doi:10.1029/2009JA014661.

Mishin, E., and M. Banaszkiewicz (1998), On auroral ion conics and electron beams acceleration, *Geophys. Res. Lett.*, *25*(23), 4309–4312, doi:10.1029/1998GL900165.

Mishin, E. V., and M. Förster (1995), "Alfvénic shocks" and low-altitude auroral acceleration, *Geophys. Res. Lett.*, *22*(13), 1745–1748.

Mishin, E. V., and K. Schlegel (1994), On incoherent-scatter plasma lines in aurora, *J. Geophys. Res.*, *99*(A6), 11391–11399.

Robinson, P. A. (1997), Nonlinear wave collapse and strong turbulence, *Rev. Mod. Phys.*, *69*, 507–573.

Sedgemore-Schulthess, F., and J.-P. St. Maurice (2001), Naturally enhanced ion-acoustic spectra and their interpretation, *Surv. Geophys.*, *22*, 55–92, doi:10.1023/A:1010691026863.

Semeter, J., and E. M. Blixt (2006), Evidence for Alfvén wave dispersion identified in high-resolution auroral imagery, *Geophys. Res. Lett.*, *33*, L13106, doi:10.1029/2006GL026274.

Semeter, J., M. Zettergren, M. Diaz, and S. Mende (2008), Wave dispersion and the discrete aurora: New constraints derived from high-speed imagery, *J. Geophys. Res.*, *113*, A12208, doi:10.1029/2008JA013122.

Sotnikov, V., et al. (1996), Generation of auroral radio waves by a gyrating electron beam, *Eos. Trans. AGU*, *77*(46), F544, Fall Meet. Suppl., Abstract SA31B-11.

Stubbe, P., H. Kohl, and M. T. Rietveld (1992), Langmuir turbulence and ionospheric modification, *J. Geophys. Res.*, *97*(A5), 6285–6297, doi:10.1029/91JA03047.

Weatherwax, A. T., J. LaBelle, and M. L. Trimpi (1994), A new type of auroral radio emission observed at medium frequencies (∼1350–3700 kHz) using ground-based receivers, *Geophys. Res. Lett.*, *21*(24), 2753–2756, doi:10.1029/94GL02512.